

Computer Simulation of the Mechanical Behaviour of Implanted Biodegradable Stents in a Remodelling Artery

ENDA L. BOLAND,^{1,2} JAMES A. GROGAN,¹ CLAIRE CONWAY,¹
and PETER E. MCHUGH¹

1.—Biomechanics Research Centre, Biomedical Engineering, College of Engineering and Informatics, National University of Ireland Galway, Galway, Ireland. 2.—e-mail: e.boland1@nuigalway.ie

Coronary stents have revolutionised the treatment of coronary artery disease. While coronary artery stenting is now relatively mature, significant scientific and technological challenges still remain. One of the most fertile technological growth areas is biodegradable stents; here, there is the possibility to generate stents that will break down in the body once the initial necessary scaffolding period is past (6–12 months) (Grogan et al. in *Acta Biomater* 7:3523, 2011) and when the artery has remodelled (including the formation of neo-intima). A stent angioplasty computational test-bed has been developed by the authors, based on the Abaqus software (DS-SIMULIA, USA), capable of simulating stent tracking, balloon expansion, recoil and in vivo loading in atherosclerotic artery model. Additionally, a surface corrosion model to simulate uniform and pitting corrosion of biodegradable stents and a representation of the active response of the arterial tissue following stent implantation, i.e. neointimal remodelling, has been developed. The arterial neointimal remodelling simulations with biodegradable stent corrosion demonstrate that the development of new arterial tissue around the stent struts has a substantial effect on the mechanical behaviour of degrading stents.

INTRODUCTION

Stents have revolutionised the treatment of arterial disease. Acting as a supporting scaffold, these small mesh devices are now routinely inserted into arteries where the blood flow has become dangerously restricted. While coronary artery stenting is now relatively mature, significant scientific and technological challenges still remain. Overall, however, the revolutionary success of coronary artery stenting has led to the emergence of stenting technology for the carotid, neural and peripheral vasculature. The adaptability of the stent concept has opened horizons beyond the vasculature, with stent technology now being developed for, amongst others, pulmonary, gastro-intestinal and structural heart applications (e.g. transcatheter aortic valve implantation stents).

In relation to coronary stents, one of the most fertile technological growth areas is biodegradable stents; here, there is the possibility to generate stents that will break down in the body once the

initial necessary scaffolding period is past (6–12 months)¹ and when the artery has remodelled (including the formation of neointima). This brings advantages including the possibly of reduced risk of in-stent restenosis and late stent thrombosis,² and the restoration of vasomotion potential. This is a very exciting technology, and stents based on both metal and polymer platforms are emerging.^{3,4}

From the perspective of stent design, the phenomenon of biodegradation, through either surface degradation in the case of metals¹ or bulk degradation in the case of polymers,⁵ adds complication to the analysis, design and development process, in comparison to that for permanent stents. Today, a problem is that stent developers must rely on feedback from animal trials in order to gauge in vitro–in vivo correlation (IVIVC) and guide design. This is expensive and time consuming. Our aim is to improve the process of IVIVC through the development of an effective implant lifetime simulation. Here, a method to simulate the degradation of metal stents (magnesium alloy) is summarised,

and implications for stent scaffolding performance presented. Stent degradation, in the context of a remodelling artery, is then simulated to explore how neointimal remodelling influences the mechanics of a degrading stent.

METHODS

Corrosion Models

A stent angioplasty computational test-bed has been developed by the authors, based on the Abaqus software (DS-SIMULIA, USA), capable of simulating stent tracking, balloon expansion, acute recoil and in vivo loading,^{1,2,6,7} in an atherosclerotic artery model. Additionally, a surface corrosion model has been developed and calibrated against experimental corrosion data for magnesium (Mg) alloy AZ31,¹ and implemented in Abaqus/Explicit using a Biotronik Magic stent geometry. This model takes two forms, and in both cases, material removal through corrosion is simulated by individual element removal from the finite element mesh. First, a *uniform corrosion* form, where surface corrosion is assumed to occur homogeneously and at a uniform rate over the surface of a sample/component. In this case, the model degradation rate is the same for all surface elements in the finite element mesh and is calibrated directly from the experimentally measured macroscopic degradation rate for the AZ31 samples.¹ Therefore, one parameter, the nominal degradation rate, k_U (h^{-1}), is determined. Second, a *pitting corrosion* form, where the degradation rate for all surface elements is not the same, and where the probability of any surface element being removed is determined by a Weibull distribution function.¹ Tuning the Weibull parameter allows for a range of phenomenology to be captured, from a relatively uniform degradation to a highly localized and “pitting” degradation, the latter being quite characteristic of Mg alloys in corrosive media (e.g. Hank’s solution). In this model, once a pit has been nucleated through the removal of a surface element, the rate of the neighbouring element removal is controlled by a further parameter (a pit growth rate

parameter). Therefore for this model, three parameters (nominal degradation rate, k_U (h^{-1}), Weibull function parameter, γ , and growth rate parameter, β) must be determined. These parameters are calibrated and model performance validated against data generated in independent corrosion and corrosion with loading experiments performed on Mg AZ31.¹ The model (in both forms) has been implemented in the previously described computation test-bed and used for stent analysis and design simulations.

Uniform Corrosion in Remodelling Artery

The original computational test-bed is limited in its representation of the active response of the arterial tissue following stent implantation, i.e. neointimal remodelling. Consequently, the test-bed has been enhanced to incorporate a representation of neointimal tissue growth driven by stress through a continuum damage formulation, based on the work of Lally and Prendergast.⁸ The process is implemented in Abaqus software through a thermal analogy formulation. The arterial lumen is filled with a mesh of deactivated elements a “ghost mesh”, with negligible initial mechanical properties (see Fig. 1). Maximum principal stress in the artery due to stent deployment is used to generate a damage parameter D , which acts like a source term that results in a diffusion of cells into the ghost mesh. If the concentration of cells in a small region or element is denoted n , the change in the cell concentration $\frac{dn}{dt}$, is computed by;

$$\frac{dn}{dt} = k\nabla^2 n + cD,$$

where k is the diffusion coefficient of cells into arterial tissue, ∇^2 is the Laplace operator, D is the damager parameter and c is a constant which relates the damage parameter to cell proliferation rate. Elements in the ghost mesh become activated (assigned tissue mechanical properties) when the local cell concentration reaches a threshold level.

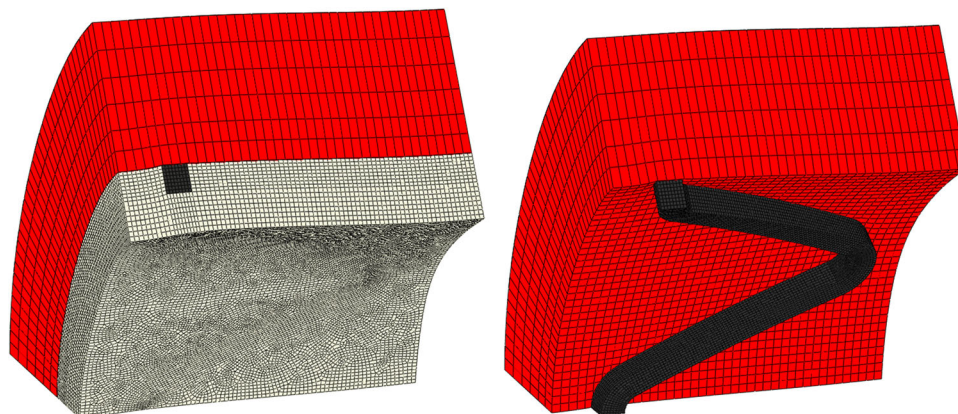


Fig. 1. Finite element model for stent degradation in a remodelling artery with artery (red), stent strut (black) and ghost mesh (grey).

The thickness of the ghost mesh was selected as 0.32 mm based on average maximal neointimal thickness values reported for the Biotronik 1st generation DREAMS stent 6 months after implantation.⁹ This thickness is important as it controls the maximum amount of neointimal remodelling that may occur during the simulation. Elastic incompressible properties are assigned to the new neointimal tissue in accordance with Lally and Prendergast⁸ who approximated the stiffness of arterial tissue under low loads as 1 MPa. Stiffness properties of the deactivated ghost mesh were also initially taken from Lally and Prendergast (0.05 MPa).⁸ Minimising this parameter is essential to ensure that the deactivated elements have negligible effect on the results on the model; however, too low a value can cause finite element-related issues such as mesh distortion and crashing of the simulation. It was found that a lower stiffness value of 0.01 MPa for the deactivated ghost mesh provided optimum balance between minimising the effect the deactivated ghost mesh has on results of the model without causing distortion of the mesh. Thus, this value was used throughout the analysis.

The stent is modelled using Mg AZ31 alloy where elasticity is considered linear and isotropic and described through Young's modulus and Poisson's ratio, while plasticity is described using J_2 flow theory and non-linear isotropic hardening. The stent geometry is a representation of the Biotronik 2nd generation DREAMS stent with a thickness of 150 μm .¹⁰ A detailed review on degradation models previously applied to both metallic and polymeric stents is given in Boland et al.¹¹

The degradation model used in this study is an adapted version of Grogan et al.'s¹ uniform corrosion model. The uniform model was selected over the pitting corrosion model as it provides a more desirable corrosion mechanics. In the model from Ref. 1 the elements on the exterior surface of the stent which would be either exposed to the flowing corrosive environment or touching the arterial tissue are selected as part of the initial corrosion surface. The elastic and plastic properties of the elements on the corrosion surface are linearly reduced with increasing damage. When an element on the corrosion surface is completely damaged, it is removed from the simulation. Subsequently, the corrosion surface is automatically updated using an element connectivity map to contain the new elements that would now be exposed to the corrosive environment. In the uniform corrosion case, this effectively results in a layer-by-layer corrosion development beginning on the exterior surface and ending at the centre of the stent.

In the model implemented here, Grogan et al.'s¹ uniform corrosion model is adapted to exclude element deletion when an element is completely damaged. Instead, completely damaged elements are modelled as a magnesium corrosion product which is assumed to be a soft elastic incompressible material.

A three-layer artery of inner diameter 3.0 mm, with artery layer thicknesses taken from the work of Holzapfel et al.,¹² is modelled using an isotropic reduced sixth-order hyperelastic material model, with model parameters taken from Gervaso et al.,¹³ based on experimental tissue testing by Holzapfel et al.¹²

Due to complexities in creating the ghost mesh of deactivated elements, the deployment of the stent was not explicitly simulated. To create the condition in the computational simulation where the stent is providing scaffolding support to the artery, a different method is used which has been used previously in other studies.⁸ The initial geometry of the stent is approximated as that of an expanded stent. A 10% axial stretch and pressure load is applied to the internal surface of the artery. Subsequently, the artery is moved over the stent and the pressure load on the artery is removed allowing the artery to relax onto the stent. While this approach for creating the condition of a stent providing scaffolding support to the artery neglects the plastic deformation in the stent due to deployment, it is consistent with corrosion modelling approach of¹ which in the present form is not explicitly strain- or stress-modulated. This method was considered acceptable for this study as it is focused on stent degradation mechanics and neointimal remodelling of the artery following stent implantation.

Abaqus/Explicit (DS-SIMULIA) solver coupled with VUSDFLD and VUAMP subroutines was used in this analysis. To minimise dynamic effects, the Rayleigh damping coefficient was applied to shell elements on the external surface of the artery and internal surface of ghost mesh. This parameter ensures that unrealistic diameter fluctuations are avoided through energy dissipation⁶ and that the ratio of kinetic to internal energy is maintained below 5% for quasi-static analysis.

An initial parameter study was conducted to determine the effects stent degradation rates, material properties of stent corrosion products and

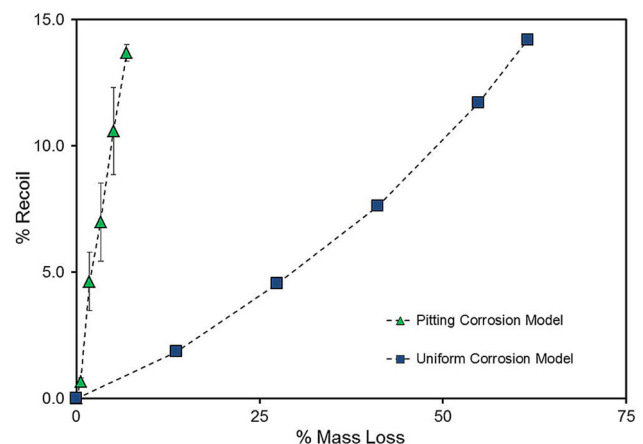


Fig. 2. Percentage stent recoil as a function of Mg mass loss for degradation of Biotronik Magic Mg stent in an atherosclerotic artery model. Image reproduced with permission¹.

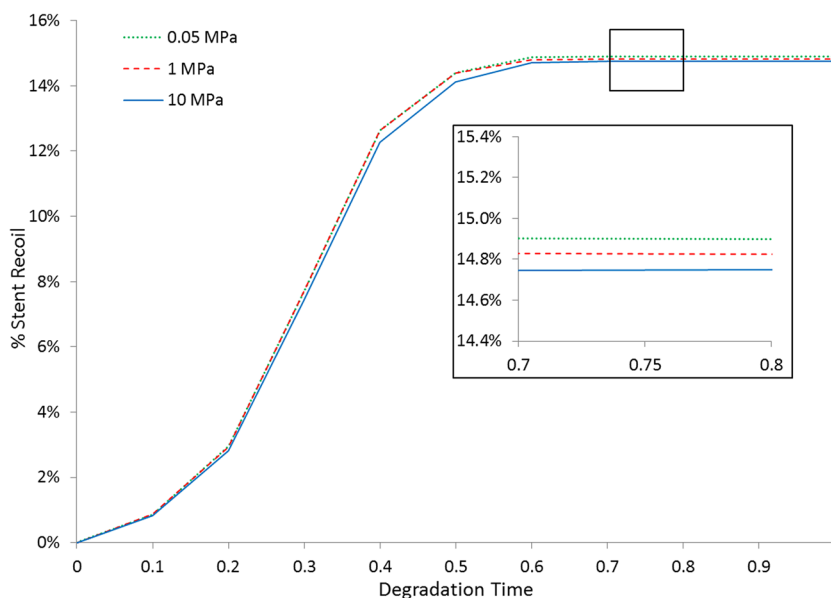


Fig. 3. Analysing the effect Mg corrosion product properties has on stent recoil rates (fast degradation no remodelling).

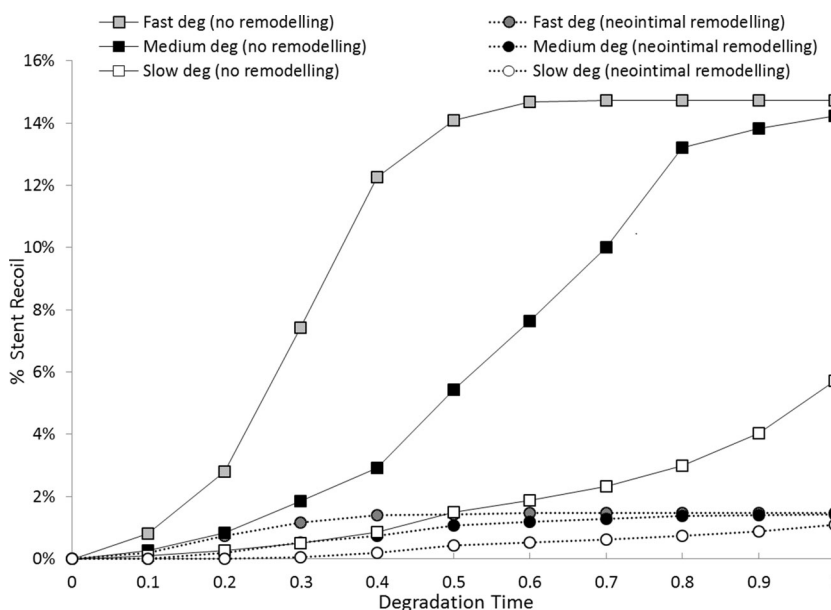


Fig. 4. Percentage stent recoil versus normalised degradation time in an artery with and without neointimal remodelling.

material properties of new neointimal tissue has on the arterial scaffolding support provided by the biodegradable magnesium stent.

RESULTS AND DISCUSSION

The first main result of the simulations is that, when applied to a Biotronik Magic Mg stent design in the computational test-bed, the pitting corrosion model predicts a scaffolding support loss rate (stent recoil) that is significantly higher than that of the uniform corrosion model (see Fig. 2).

One implication here is that it would be much more desirable to have a stent that corroded in a more uniform way to achieve better scaffolding support over time. This more favourable uniform corrosion behaviour is assumed for the remainder of the study.

The values of elastic modulus of magnesium corrosion product were varied for the scenario which causes maximum stent recoil rates (fast degradation no neointimal remodelling). The properties of magnesium corrosion product only have a minor effect on recoil rates of the degrading stent as illustrated

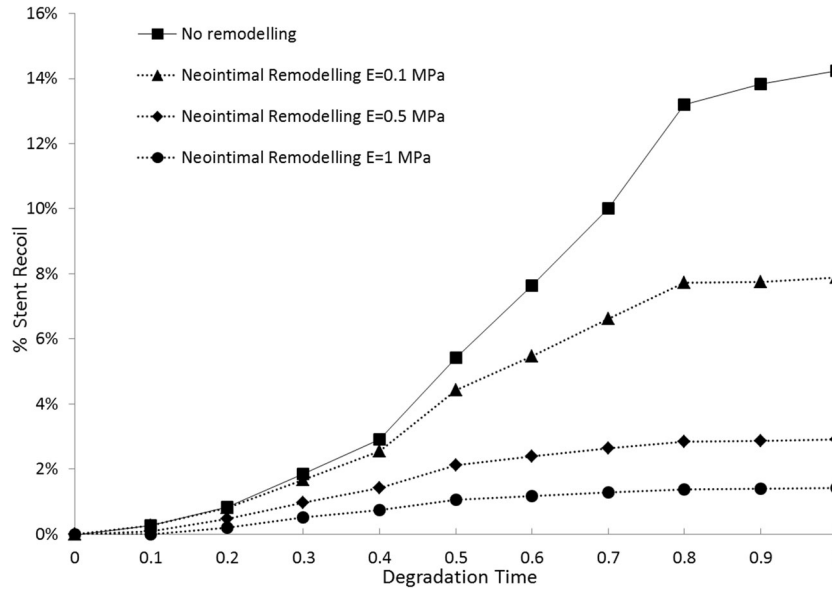


Fig. 5. Analysing the effect neointimal tissue properties has on stent recoil rates (medium degradation).

in Fig. 3. An elastic modulus of 10 MPa results in final stent recoil rate of 14.75%, while elastic modulus values of 1 MPa and 0.05 MPa result in total recoil rates of 14.8% and 14.9%, respectively.

The effect that stent degradation at various rates (fast, medium and slow) has on the recoil rates of a completely remodelled artery ($E = 1$ MPa) and an artery without any neointimal remodelling was simulated. The results are illustrated in Fig. 4.

The results show that neointimal remodelling has a significant effect on the mechanics of the degrading stent. Without neointimal remodelling as the stent degrades, it loses its mechanical integrity and the stent cannot maintain scaffolding support to the artery, which is illustrated in Fig. 4 by the increase in stent recoil as the degradation proceeds. However, if the stent is degrading in a fully remodelled artery, stent recoil is significantly less. In this case, as the stent degrades, the load from the artery is redistributed from the stent to the new neointimal tissue. This redistribution of load allows scaffolding support of the artery to be maintained even for a completely degraded stent.

In a further analysis, the properties of the neointimal tissue were varied for the same stent degradation rate to quantify the effect that it has a stent recoil rate. The initial neointimal stiffness value of 1 MPa⁸ was reduced first to 0.5 MPa and then to 0.1 MPa, with the results shown in Fig. 5. The lower values of 0.5 MPa and 0.1 MPa were chosen to explore the critical dependence of the results on the neointimal tissue properties given that diseased arterial tissue properties are highly variable.¹⁴

Figure 5 demonstrates that the elastic properties of the new neointimal tissue are the dominant parameter which controls stent recoil rate in the model. Stent recoil at the end of the degradation simulation changes

from 7.9% to 2.9% to 1.4% depending on the selected stiffness value of the neointimal tissue (1 MPa, 0.5 MPa or 0.1 MPa, respectively).

CONCLUSION

The corrosion simulations clearly demonstrate the critical importance of the fundamental corrosion behaviour of the material determining the overall stent performance. Specifically, the severe negative effects of pitting corrosion are demonstrated and quantified (Fig. 2). The clear message here is that, while biodegradable metal stents have the potential for significant clinical impact, efforts need to be focused on alloy and production method development to eliminate/reduce the pitting tendency, and to retard overall degradation rates for the magnesium stent application. However, it is acknowledged that retardation of the pitting corrosion is not as critical in other implant applications. Having said that, significant improvements in biodegradable metal stent performance can be achieved through stent geometry optimisation, as demonstrated in Ref. 2 with a factor of 2 in stent radial strength being achievable.

Although it has been shown that corrosion product is present in arterial tissue following degradation of Mg stents,¹⁵ the results of these degradation simulations (Fig. 3) show that it has little effect on recoil rates of the degrading stent. This may be due to the entire range of assumed properties of magnesium corrosion product ($E = 0.05$ –10 MPa) being a fraction of the elastic modulus of undamaged Mg AZ31 ($E = 44,000$ MPa). Therefore, these computational results suggest the use of element deletion for completely damaged elements in the uniform and pitting corrosion models of Grogan et al.¹ would not introduce inaccuracies into the results.

The first phase of simulations ignored the active arterial tissue remodelling that occurs on stent implantation, including for biodegradable stents. The second phase of simulations, i.e. the arterial neointimal remodelling simulations with biodegradable stent, highlight how the development of new arterial tissue around the stent struts has a substantial effect on the mechanical behaviour of degrading stents (Fig. 4). Furthermore, the material properties of the new neointimal tissue significantly affect stent recoil rates (Fig. 5), thus correct representation of in vivo properties is essential to ensure accuracy of the model. The relative volumes of the stent to new neointimal tissue may explain the reason behind the importance of neointimal tissue properties over magnesium corrosion product properties in this model.

Further model development, parameter studies and experimental validation are clearly required here; nevertheless, this result could contribute to the explanation as to why biodegradable metal stents degrade and lose scaffolding capability more slowly in vivo (where tissue remodelling is occurring) in comparison to in vitro.^{1,16} A significant overall conclusion of the work thus far is that a method has been developed that allows for *quantitative* prediction of the short- and long-term mechanical performance of biodegradable metal stents, as a function of the material properties and fundamental material corrosion behavior, and as such should be of value to stent developers.

ACKNOWLEDGEMENTS

The authors would like to acknowledge funding from the Irish Research Council for Science, Engi-

neering and Technology and the SFI/HEA Irish Centre for High-End Computing (ICHEC) for the provision of computational facilities and support.

REFERENCES

1. J.A. Grogan, B.J. O'Brien, S.B. Leen, and P.E. McHugh, *Acta Biomater.* 7, 3523 (2011).
2. J.A. Grogan, S.B. Leen, and P.E. McHugh, *Biomaterials* 34, 8049 (2013).
3. N. Patel and A.P. Banning, *Heart* 99, 1236 (2013).
4. M. Haude, R. Erbel, P. Erne, S. Verheye, H. Degen, D. Bose, P. Vermeersch, I. Wijnbergen, N. Weissman, F. Prati, R. Waksman, and J. Koolen, *Lancet* 9, 836 (2013).
5. R.N. Shirazi, F. Aldabbagh, A. Erxleben, Y. Rochev, and P. McHugh, *Acta Biomater.* 10, 4695 (2014).
6. C. Conway, F. Sharif, J.P. McGarry, and P.E. McHugh, *Cardiovasc. Eng. Technol.* 3, 374 (2012).
7. C. Conway, J.P. McGarry, and P.E. McHugh, *Ann. Biomed. Eng.* 42, 2425 (2014).
8. C. Lally and P.J. Prendergast, *Mechanics of Biological Tissue*, ed. G. Holzapfel and R. Ogden (Heidelberg: Springer, 2006), p. 255.
9. R. Waksman, F. Prati, N. Bruining, M. Haude, D. Böse, H. Kitabata, P. Erne, S. Verheye, H. Degen, P. Vermeersch, L. Di Vito, J. Koolen, and R. Erbel, *Circ. Cardiovasc. Interv.* 6, 644 (2013).
10. H. Kitabata, R. Waksman, and B. Warnack, *Cardiovasc. Revasc. Med.* 15, 109 (2014).
11. E.L. Boland, R. Shine, N. Kelly, C.A. Sweeney, and P. E. McHugh, *Ann. Biomed. Eng.* (2015). doi:10.1007/s10439-015-1413-5.
12. G.A. Holzapfel, G. Sommer, C.T. Gasser, and P. Regitnig, *Am. J. Physiol. Heart Circ. Physiol.* 289, H2048 (2005).
13. F. Gervaso, C. Capelli, L. Petrini, S. Lattanzio, L. Di Virgilio, and F. Migliavacca, *J. Biomech.* 41, 1206 (2008).
14. M.T. Walsh, E.M. Cunnane, J.J. Mulvihill, A.C. Akyildiz, F.J.H. Gijssen, and G.A. Holzapfel, *J. Biomech.* 47, 793 (2014).
15. M. Maeng, L.O. Jensen, E. Falk, H.R. Andersen, and L. Thuesen, *Heart* 95, 241 (2009).
16. J.E. Schaffer, Ph.D. thesis, Purdue University, Indiana, 2012.